MPPT control of PV array based on PSO and adaptive controller

Totok Winarno[1], Lucky Nindya Palupi[2], Agus Pracoyo[3], Lunde Ardhenta[4]
[1,2,3]Department of Electrical Engineering, State Polytechnic of Malang, Indonesia
[4]Department of Electrical Engineering, Brawijaya University, Indonesia

Article Info	ABSTRACT
	In general, Photovoltaic (PV) array is not able to generate maximum power automatically, because some partial shading caused by trees, clouds, or buildings. Irradiation imperfections received by the PV array are overcome by applying maximum power point tracking (MPPT) to the output of the PV array. In order to overcome these partial shading problems, this system is employing particle swarm optimization (PSO) as MPPT method. It optimizes the output power of the solar PV array by Zeta converter. Output voltage of MPPT has high rate such that it needs stepdown device to regulate certain voltage. Constant voltage will be the input voltage of buck converter and controlled using adaptive PID. Adaptive control based on model reference adaptive control (MRAC) has design that almost same as the conventional PID structure and it has better performance in several conditions. The proposed system is expected to have stable output and able to perfectly emulate the response of the reference model. From the simulation results, it appears that PSO have high tracking accuracy and high tracking speed to reach maximum power of PV array. In the output voltage regulation, adaptive control does not have a stable error status and consistently follows the set point value. *This is an open access article under the [CC BY-SA](#) license.*

Corresponding Author:

Totok Winarno,
Department of Electrical Engineering,
State Polytechnic of Malang,
Soekarno Hatta St. 9 Malang 65144, Indonesia.
Email: totok.winarno@polinema.ac.id

1. INTRODUCTION

The utilization of electricity represents economic and social development in every country. Energy resources, environmental pollution, global warming, and energy inefficiency are big issues in dany countries. Most of researchers around the world are studying renewable resources, such as PV [1-3]. PV generally cannot work directly at its maximum power, because the PV operating voltage mostly follow the battery voltage connected to the PV. Therefore, the application of maximum power point tracking (MPPT) must be used to regulate PV module in order to achieve Maximum Power Point (MPP) [4-6]. Commonly problem in PV that are connected in an array is the different level of irradiation. Some of them may be covered in shadows caused by trees, clouds, or other objects. The power generated from each PV module becomes nonuniform, such that the total output power will be less than maximum power and it causes multi-peak on the PV characteristic curve [7-11].

Many researchers have developed various MPPT methods to track MPP and overcome problems caused by partial shadows. Several methods [12-15] have reached an optimal solution such as fuzzy logic, neural network, firefly algorithm, and other metaheuristic algorithm. An examination concept of metaheuristic is employed as an optimization problem without defining a definite objective function. Particle Swarm Optimization (PSO) can obtain global peaks by utilizing randomization to avoid trapping algorithms at local peak [16-18].

In order to regulate constant voltages, the robust controller is needed [19-21]. The maximum power value obtained by MPPT is not able to be set as output value of the system because the output voltage is extremely unstable. The other DC converter is used to keep and maintain the output voltage according to the reference value. DC-DC converters are a real form of DC voltage regulators for step up, step down, or both. System dynamics are needed to design controllers that are able to achieve the desired value. PID control is widely applied in the industrial world with a variety of adjustment techniques [22, 23]. One of the adaptive techniques is that Model Reference Adaptive Control (MRAC) has succeeded in increasing the system response rather than the fixed parameter PID controller [24, 25] by providing a reference model followed by the system response. MIT rules are used in this study to determine adaptive PID parameters [26]. Therefore, the main objective of this research is to emphasize how to design an MPPT system that has a constant output voltage.

2. RESEARCH METHOD

This research is using metaheuristic algorithms for MPPT to generate maximum power in PV arrays under partial shadow conditions. PSO as MPPT method and adaptive control based on MRAC are the theory used to compose this research.

2.1. PV array model

PV cells are defined as technologies that produce DC power supplies with light effect. As long as the semiconductor material acquires sunlight, the PV cell will always generate electricity and the PV cell will stop producing electricity when there is no received sunlight. Exponential equations for modeling photovoltaic cells are derived from the physical laws for pn junction and are generally accepted as representations of PV cell characteristics indicated by (1).

$$I = I_{ph} - I_s \left(exp \frac{q(V+IR_S)}{NKT} - 1 \right) - \left(\frac{(V+IR_S)}{R_{sh}} \right) \tag{1}$$

where I_{ph} is the current generated by the diode, I_s is the reverse saturation current of the diode, q is the electron charge with the value of 1.602×10^{19} Coulombs, T is the cell temperature in Kelvin, N is the dimensionless diode ideality factor as measure of how closely the diode follows the ideal diode (1) and k is the Boltzmann constant with the value of $38 \times 10^{-23} J/K$. PV equivalent circuits can be specified as given in Figure 1.

The output of PV modules is strongly influenced by environmental conditions, namely solar radiation and cell temperature. As shown in (2) shows the current equation generated by photons, I_{ph}.

$$I_{ph} = [I_{SC} + k_1(T - 298)] \frac{\lambda}{100} \tag{2}$$

where I_{SC} is the cell short-circuit current at 25°C, K_I is coefficient of short circuit current temperature, and λ is the solar radiation in W/m^2. Temperature changes in PV modules can affect short circuit currents, I_{sc}, as shown by (2) and saturation currents of diodes, I_s, and as indicated by (3).

$$I_s(T) = I_s \left[\frac{T}{T_{nom}} \right]^3 exp \left[\left(\frac{T}{T_{nom}} - 1 \right) \frac{E_g}{NV_t} \right] \tag{3}$$

where I_s is the reverse saturation current, E_g is the band gap energy semiconductor in V, and V_t is the terminal voltage of solar cell in 25°. Low voltages generated PV cell is not enough to be used commercially, therefore, photovoltaic cells are integrated and connected in a module to produce the least voltage that can be used to charge 12 volt batteries [8]. The PV array is a series and/or parallel combination of several PV modules. The I-V curve of the PV arrangement is a curve with a larger scale than the I-V curve of a single module, as illustrated in Figure 2.
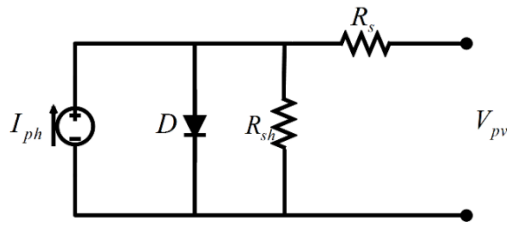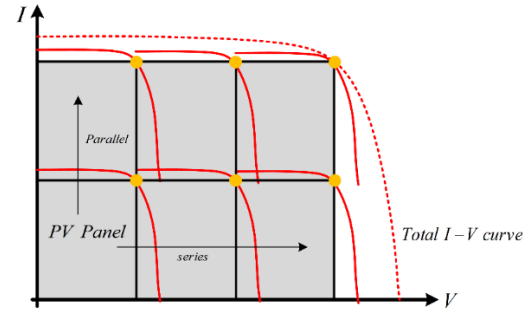
Figure 1. Equivalent circuit of PV cell

Figure 2. PV array curves that are formed from
a series-parallel arrangement of PV modules

2.2. MPPT-particle swarm optimization

The variable controlled by MPPT is the reference voltage generated by the DC converter, so the particle position is V_{ref} and the best value is PV (P) compared to that position. Some PSO variables that are converted to PV systems can be seen in Table 1.

Table 1. PSO variables to PV systems

PSO	PV Systems
Particle Position (P_i)	Reference voltage (V_{ref})
Particle speed (V_i)	The range of voltage increase when the particle moves
The best fitness value of particles	The best power of particles ($P_{best,i}$)
The best position of particles ($P_{best,i}$)	The voltage that produces the best particle power ($V_{best,i}$)
The best global fitness value	Global best power (P_{Gbest})
Global best position (G_{best})	The voltage that produces the best global power (V_{Gbest})

The first step to start the PSO algorithm is to determine the value of the parameters used in the PSO algorithm, namely the number of particles (N), the weight of inertia (W), cognition-only learning factor (C_1), and social-only learning factor (C_2). The second step is to initialize the stress value and the initial velocity of the particle. The initial particle voltage is arranged randomly in the search space where it is possible to fine local peak. Particle velocity in this PV system is the range of voltage increases when the particle moves. The velocity of each particle is given an initial value of zero, then the velocity will vary according to the particle velocity equation for PSO (4) and (5).

$$V_i^{j+1} = W \times V_i^j + C_1 \times rand_1 \times \left(P_{best,i} - P_i^j\right) + C_2 \times rand_2 \times \left(G_{best} - P_i^j\right) \tag{4}$$

$$P_i^{j+1} = V_i^{j+1} + P_i^j \tag{5}$$

The next step is to multiply the voltage (V) and current (I) of each particle in order to obtain the power (P). The recent power will be compared with the previous best power (P_{best}) that has been saved by the particle. If the particle power is higher than P_{best}, then the value of P_{best} will be replaced by the value of P, as well as the voltage that produces P_{best} will be replaced by V particles. When the initial iteration does, the particle does not have the P_{best} saved previously, so the current particle power automatically becomes the initial P_{best} value of the particle. Then, the best value of the particles will be compared with the best value of the group. If the best value of particles is higher, then the best value of the group will be replaced by that value. But if there is no changed, the best value of the group will remain the same. This step is carried out by 5 particles one by one alternately.

After getting the best particle values and the best group values, the voltage and velocity of each particle are updated using the PSO equation. The convergence criteria is the difference between the best power and the power of each particle is zero and less than ε_1. In this condition, the algorithm stops at the maximum point. However, if it is not met, then the algorithm will repeat the calculation of the power of each particle to reach the maximum point.

2.3. Buck converter

The configuration of buck converter is shown in Figure 3. The desired output voltage is a step-down voltage which is generated by the Pulse width modulation (PWM). PWM sets the ignition on the buck converter switch based on the duty cycle value. In this study, buck converter operates in CCM (continuous conduction mode) so that the inductor current is always greater than zero. The advantages of buck configuration are high efficiency, simple circuit, no need for transformers, low stress level on switch components, and small ripple at the output voltage, furthermore, the filter needed is relatively small. The buck converter circuit does not have an isolation component to maintain the system between input and output. The switch ON state and OFF state are depicted in Figure 4.
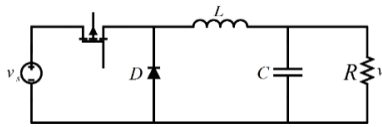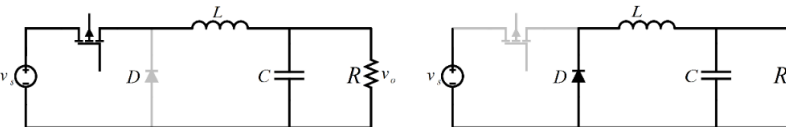

Figure 3. Buck converter   Figure 4. Buck converter when switch is ON and switch is OFF

The vector x have two parameters, x_1 is represented as the inductor current i_L and x_2 is represented as the capacitor voltage v_C. When the switch is ON, the derivative of x_1 and x_2 are defined in (6) and (7) respectively. Now the derivative of x_1 and x_2 when the switch is OFF are presented in (8) and (9). The state space averaged model is obtained by combining the ON and OFF condition, the mathematical expression for buck converter is shown in (10).

$$\dot{x}_1 = -\frac{1}{L}x_2 + \frac{1}{L}V_{in} \tag{6}$$

$$\dot{x}_2 = \frac{1}{C}x_1 - \frac{1}{RC}x_2 \tag{7}$$

$$\dot{x}_1 = -\frac{1}{L}x_2 \tag{8}$$

$$\dot{x}_2 = \frac{1}{C}x_1 - \frac{1}{RC}x_2 \tag{9}$$

$$\begin{bmatrix} \dot{x}_1 \\ \dot{x}_2 \end{bmatrix} = \begin{bmatrix} 0 & -\frac{1}{L} \\ \frac{1}{C} & -\frac{1}{RC} \end{bmatrix} \begin{bmatrix} x_1 \\ x_2 \end{bmatrix} + \begin{bmatrix} \frac{d}{L} \\ 0 \end{bmatrix} V_{in} \tag{10}$$

2.4. Adaptive control

The PID controller has a simple structure so that this controller is easy to apply in many systems. However, the PID parameter has a character that is suitable for setting system with a single input and has a single output (SISO) and therefore not able to compensate various conditions in the actual environment. Designing an adaptive control according to reference model (MRAC) is one type of adaptive control structure by developing adaptation parameters for PID control using certain rules. The block diagram in Figure 5 shows the structure of the MRAC. The Buck converter uses one inductor and one capacitor, which means this system is a 2nd order system. The system model is described as:

$$\frac{Y_p(s)}{U(s)} = \frac{b}{s^2 + a_1 s + a_2} \tag{11}$$

The second-order reference model given by:

$$\frac{Y_m(s)}{U(s)} = \frac{bm_1 s^2 + bm_2 s + bm_3}{s^3 + am_1 s^2 + am_2 s + am_3} \tag{12}$$

The adaptation error:

$$\varepsilon = Y_p - Y_m \tag{13}$$

The cost function is denoted as:

$$J(\theta) = \frac{\varepsilon^2(\theta)}{2} \tag{14}$$

where ε is the difference between the output system and the output model reference or error. MIT rule is employed in this adaptive control design, the change in error respects to the parameter θ and the change in parameter θ respects to time can determine the value of the cost function to be close to zero so that it obtains the same value as the reference value. γ is a definite positive value that indicates the adaptability of the controller.

$$\frac{d\theta}{dt} = -\gamma \frac{\partial J}{\partial \theta} = -\gamma \varepsilon \frac{\partial \varepsilon}{\partial \theta} \tag{15}$$

$$\frac{dK_p}{dt} = -\gamma_p \frac{\partial J}{\partial K_p} = -\gamma \frac{\partial J}{\partial \varepsilon} \frac{\partial \varepsilon}{\partial Y_p} \frac{\partial Y_p}{\partial K_p} \tag{16}$$

where: $\frac{\partial J}{\partial \varepsilon} = \varepsilon$, $\frac{\partial \varepsilon}{\partial Y_p} = 1$. The adaptive PID controller parameters K_p, K_i, and K_d are shown in (27), (28), and (29).

$$\frac{dK_p}{dt} = -\gamma_p \frac{\partial J}{\partial K_p} = -\gamma_p \varepsilon \frac{bs}{\left(s^3 + (a_1 + bK_d)s^2 + (a_2 + bK_p)s + bK_i\right)} (R(s) - Y_p(s)) \tag{17}$$

$$\frac{dK_i}{dt} = -\gamma_i \frac{\partial J}{\partial K_i} = -\gamma_i \varepsilon \frac{b}{\left(s^3 + (a_1 + bK_d)s^2 + (a_2 + bK_p)s + bK_i\right)} (R(s) - Y_p(s)) \tag{18}$$

$$\frac{dK_d}{dt} = -\gamma_d \frac{\partial J}{\partial K_d} = -\gamma_d \varepsilon \frac{bs^2}{\left(s^3 + (a_1 + bK_d)s^2 + (a_2 + bK_p)s + bK_i\right)} (R(s) - Y_p(s)) \tag{19}$$

b, a_1, and a_2 have an unknown number, then we define $am_1 = a_1 + bK_d$; $am_2 = a_2 + bK_p$; $am_3 = bK_i$.

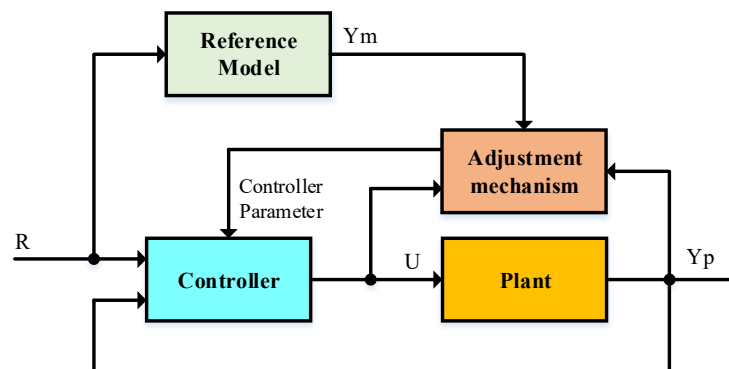Figure 5. Block diagram of a basic model reference adaptive control

3.   RESULTS AND ANALYSIS

In this system uses two converters, a zeta converter and a buck converter that connects the PV array to generate power in load demand. The zeta converter is used to obtain the maximum power of the PV array and the buck converter is used to control the output voltage at 12V. The system will be simulated according to the original conditions, starting from the PV array, zeta converter, buck converter and load as a given disturbance. The block diagram of the proposed system is illustrated in Figure 6.

In this study, using 3 PV modules installed in series as PV array. The use of PV array aims to get a graph that has a maximum of 3 peaks, two local peaks and one global peak. The SP-100-P36 is chosen for PV array modeling. The module has maximum power 60W and 36 series connected polycrystalline cells. The parameters of SP-100-P36 are provided in Table 2. In this research using the PSO method to explore the maximum power value at the output of the PV array. Some parameter for PSO are summarized in Table 3.

The output of the zeta converter is unstable at a certain value, so controller is required to make the output voltage stable. Constant voltage will be controlled using adaptive PID controller and the output voltage will be constant in setpoint. The second DC converter used in this research is buck converter. Buck converters have the following parameters, $L = 1mH$, $C = 470\mu F$, $R = 100\Omega$ and input voltage of $52V$. In this system will have two scenarios, which are a situation where the PV array is affected by the shadow or not; and the second scenario is the alteration of input voltage in buck converter. Table 4 shows MPP of each case.
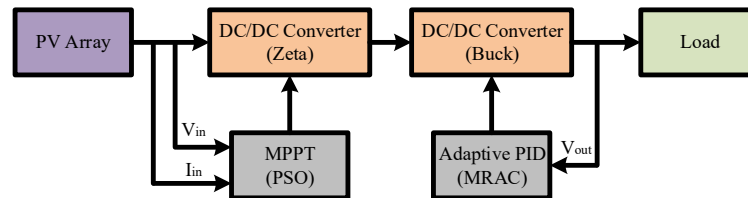

Figure 6. Block diagram system

Table 2. SP-100-P36 solar module parameters

Parameters	Value
Maximum Power (P_{max})	100 W
Voltage at Maximum Power (V_{mp})	17.6 V
Current at Maximum Power (I_{mp})	5.69 A
Open Circuit Voltage (V_{oc})	22.6 V
Short Circuit Current (I_{sc})	6.09 A

Table 3. PSO parameters

Parameter	Value
Particle number (N)	5
Inertia weight (W)	0.4
Cognition-only learning factor (C_1)	0.2
Social-only learning factor (C_2)	0.8
Tolerance value (ε_1)	1

Table 4. MPP in several case

Case	Iradiation (W/m^2)			MPP (W
	M1	M2	M3	
1	1000	1000	900	284.456
2	700	600	500	219.371

In Figure 7 and Figure 8 show the MPPT signal from the zeta converter to output voltage of buck converter experiences different partial shadows on each module. Figure 7 (a) shows the output power of MPPT accordance with the maximum power of PV is 284,456 W. There is a little error that occurs due to the determination of the parameters of the PSO that is not optimal yet. The voltage generated by the buck converter matches the desired voltage which is 12V. The same results are shown in Figure 7 (b), when the PV array gets unequal irradiatian, the maximum power value obtained is 219,371. Clearly, MMPT systems are able to achieve maximum power with tracking accuracy up to 98.76% and tracking time is less than 0.6 seconds. This shows that the designed MPPT and controller are work properly.

Because of unstable MPPT output voltage, the second converter is given some input voltage values. In order to investigate the controller is working properly, the output voltage response is presented in

Figure 8. The input voltage starts at 53V and then rises to 58 V at t = 0.2s, the response of output voltage in accordance with the desired value of 12 V. The same thing happens when the input voltage drops to 45V at t = 0.3s, the output voltage is fixed and has no overshoot at setpoint value. The proposed controller has robust and reliable response from disturbances.
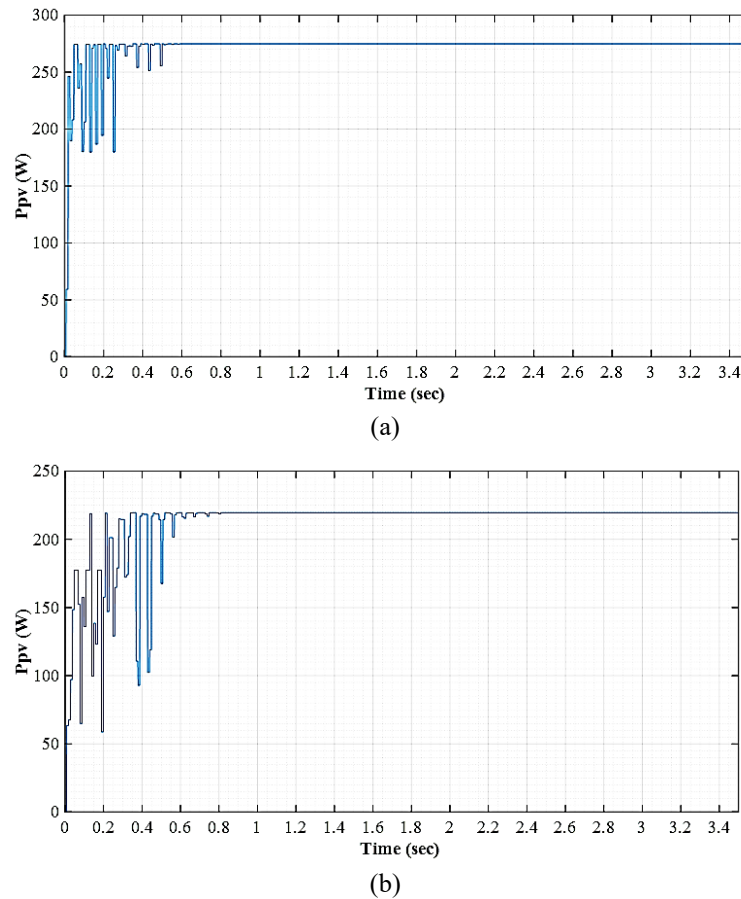

(a)

(b)

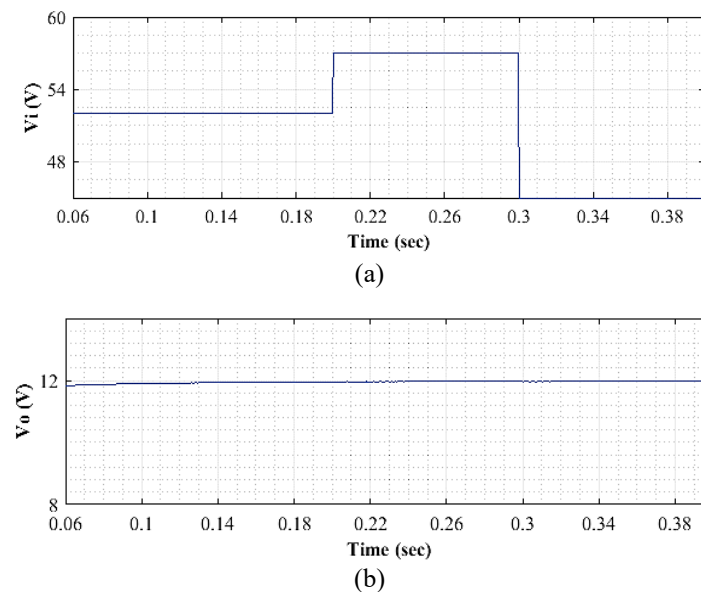Figure 7. Output power of MPPT of zeta converter in (a) case 1 and (b) case 2

(a)

(b)

Figure 8. (a) Input voltage variations, (b) Output voltage when the input voltage changes

MPPT control of PV array based on PSO and adaptive controller (Totok Winarno)

4. CONCLUSION

Output voltage of PV array have high rate voltage and unstable value. In order to find maximum power point accurately, PSO method is employed in this research. The MPPT algorithm provides constant maximum output power that always has an ever-changing value. The output voltage of the adaptive controller produces a stable output voltage. MRAC is the adaptive control structure for this research. In simulation results, high tracking accuracy and high tracking speed are working properly. It means that PSO is able to reach maximum power of PV array. The output voltage regulation using adaptive control does not have error steady state and consistently follows the reference value.

REFERENCES

[1] Chao, K. H., Chang, L. Y., & Liu, H. C., "Maximum Power Point Tracking Method Based on Modified Particle Swarm Optimization for Photovoltaic Systems," *International Journal of Photoenergy*, vol. 2013, no. 2, pp. 1-6, November 2013.

[2] J. Liu, J. Li, J. Wu, W. Zhou, "Global MPPT algorithm with coordinated control of PSO and INC for rooftop PV array," *The Journal of Engineering*, vol. 2017, no. 13, pp. 778-782, 2017.

[3] S. K. Kollimalla, M.K. Mishra, "Variable perturbation size adaptive P&O MPPT algorithm for sudden changes in irradiance," *IEEE Transactions on Sustainable Energy,* vol. 5, no. 3, pp. 718-728, July 2014.

[4] Balasubramanian, I. R., Ilango Ganesan, S., Chilakapati, N. "Impact of partial shading on the output power of PV systems under partial shading conditions," *IET Power Electronics,* vol. 7, no. 3, pp. 657-666, March 2014.

[5] M. A. M. Ramli, S. Twaha, K. Ishaque, and Y. A. Al-Turki, "A review on maximum power point tracking for photovoltaic systems with and without shading conditions," *Renewable and Sustainable Energy Reviewas*, vol. 67, pp. 144–159, January 2017.

[6] S. M. R. Tousi, M. H. Moradi, N. S. Basir, and M. Nemati, "A function-based maximum power point tracking method for photovoltaic systems," *IEEE Trans. Power Electron.*, vol. 31, no. 3, pp. 2120–2128, March 2016.

[7] L. Ardhenta, Wijono, "Photovoltaic Array Modeling under Uniform Irradiation and Partial Shading Condition," *International Journal of Applied Power Engineering (IJAPE)*, vol. 6, no. 3, pp. 144-152, December 2017.

[8] A. Badis, M. H. Boujmil, M. N. Mansouri, "A comparison of global MPPT techniques for partially shaded grid-connected photovoltaic system," *International Journal of Renewable Energy Research (IJRER)*, vol. 8, no. 3, pp. 1442-1453, September 2018.

[9] A. G. Galeano, M. Bressan, F. J. Vargas, C. Alonso, "Shading ratio impact on photovoltaic modules and correlation with shading patterns," *Energies*, vol. 11, no. 4, pp. 852, April 2018.

[10] J. Ma, T. Zhang, Y. Shi, X. Li, H. Wen, "Shading pattern detection using electrical characteristics of photovoltaic strings," *2016 IEEE International Conference on Power Electronics, Drives and Energy Systems (PEDES),* Trivandrum, pp. 1-4, 2016.

[11] A. R. Jordehi, "Maximum power point tracking in photovoltaic (PV) systems: A review of different approaches," *Renewable and Sustainable Energy Reviews*, vol. 65, pp. 1127–1138, November 2016.

[12] A. A. Elbaset, H. Ali, M. Abd-El Sattar, and M. Khaled, "Implementation of a modified perturb and observe maximum power point tracking algorithm for photovoltaic system using an embedded microcontroller," *IET Renewable Power Generation,* vol. 10, no. 4, pp. 551-560, April 2016.

[13] K. Amara et al., "Improved Performance of a PV Solar Panel with Adaptive Neuro Fuzzy Inference System ANFIS based MPPT," *2018 7th International Conference on Renewable Energy Research and Applications (ICRERA),* Paris, pp. 1098-1101, 2018.

[14] D. Haji, N. Genc, "Fuzzy and P&O Based MPPT Controllers under Different Conditions," *2018 7th International Conference on Renewable Energy Research and Applications (ICRERA)*, Paris, pp. 649-655, 2018.

[15] T. T. Yetayew, T. R. Jyothsna, G. Kusuma, "Evaluation of incremental conductance and firefly algorithm for PV MPPT application under partial shading condition," *2016 IEEE 6th International Conference on Power Systems (ICPS),* New Delhi, pp. 1-6, 2016.

[16] K. Sundareswaran, V. Vigneshkumar, P. Sankar, S. P. Simon, P. S. R. Nayak, S. Palani, "Development of an improved P&O algorithm assisted through a colony of foraging ants for MPPT in PV system," *IEEE Transactions on Industrial Informatics,* vol. 12, no. 1, pp. 187-200, Feb. 2016.

[17] D. F. Teshome, C. H. Lee, Y. W. Lin, K. L. Lian, "A modified firefly algorithm for photovoltaic maximum power point tracking control under partial shading," *in IEEE Journal of Emerging and Selected Topics in Power Electronics,* vol. 5, no. 2, pp. 661-671, June 2017.

[18] M. Dwivedi, G. Mehta, A. Iqbal, H. Shekhar, "Performance enhancement of solar PV system under Partial Shaded Condition using PSO," *2017 8th International Conference on Computing, Communication and Networking Technologies (ICCCNT)*, pp. 1-7, 2017.

[19] L. Ardhenta, et al., "Adaptive Control for Buck Converter in Hybrid Power System based on DMRAC Method," *2018 Electrical Power, Electronics, Communications, Controls and Informatics Seminar (EECCIS)*, Batu, East Java, Indonesia, pp. 282 – 286, 2018.

[20] Y. Jeung, I. Choi, D. Lee, "Robust voltage control of dual active bridge DC-DC converters using sliding mode control," *Proc. 2016 IEEE 8th International Power Electronics and Motion Control Conference (IPEMC-ECCE Asia)*, pp. 629-634, 2016.

[21] S. Oucheriah, L. Guo, "PWM-based adaptive sliding mode control for boost DC/DC converters," *2016 IEEE 8th International Power Electronics and Motion Control Conference (IPEMC-ECCE Asia)*, Hefei, 2016, pp. 629-634.

[22] K. Ang, G. Chong, Y. Li, "PID control system analysis design and technology," *IEEE Transactions on Control Systems Technology*, vol. 13, no. 4, pp. 559-576, July 2005.

[23] D. E. Seborg, T.F. Edgar and D.A. Mellichamp. "Process Dynamic and Control. 2nd edition," *Wiley*: New York, 2004.

[24] P. C. Parks. "Liapunov Redesign of Model Reference Adaptive Control Systems," *IEEE Transactions on Automatic Control*, vol. 11, no. 3, pp. 362-367, July 1966.

[25] E. Lavretsky and K. A. "Wise, Robust and adaptive control: With aerospace applications, ser. Advanced textbooks in control and signal processing," London and New York: *Springer*, 2013.

[26] M. Krstic, I. Kanellakopoulos, and P. V. Kokotovic, "Nonlinear and adaptive control design," New York: *Wiley*, 1995.

BIOGRAPHIES OF AUTHORS

Totok Winarno received B.Eng degree in Electrical Engineering from Sepuluh Nopember Instutute of Technology, Surabaya, Indonesia in 1989 and the M.Eng degrees from Brawijaya University, Malang, Indonesia in 2009. He is currently a senior lecturer in Department of Electrical Engineering, State Polytechnic of Malang, Malang, Indonesia. His research interests include embedded system and artificial intelligence.

Lucky Nindya Palupi received B.Eng degree in Electrical Engineering from Brawijaya University, Malang, Indonesia in 2011 and the M.Sc degrees from National ChiaYi University, Chiayi, Taiwan in 2014. She is currently a lecturer in Department of Electrical Engineering, State Polytechnic of Malang, Malang, Indonesia. Her research interests include digital signal processing and embedded system.

Agus Pracoyo received B.Eng degree in Electrical Engineering from Yogyakarta State University, Yogyakarta, Indonesia in 1982 and the M.Eng degrees from Brawijaya University, Malang, Indonesia in 2010. He is currently a senior lecturer in Department of Electrical Engineering, State Polytechnic of Malang, Malang, Indonesia. His research interests include embedded system.

Lunde Ardhenta was born in East Java Province, Indonesia, in 1988. He is currently a junior lecturer at Department of Electrical Engineering, University of Brawijaya, Indonesia. He received the M.S. degree in Department of Electrical Engineering, National ChiaYi University, Taiwan in 2015. He completed his Bachelor degree in Department of Electrical Engineering, University of Brawijaya, Indonesia in 2011. His research interests include renewable energy applications, linear control and digitalized control techniques, and power electronics.